






Transcriptomic Cross-Species Analysis of Chronic Liver Disease Reveals Consistent Regulation Between Humans and Mice

Christian H. Holland ^{1,4}, Ricardo O. Ramirez Flores ^{1,2}, Maiju Myllys ⁴, Reham Hassan,^{4,5} Karolina Edlund,⁴ Ute Hofmann,⁶ Rosemarie Marchan,⁴ Cristina Cadenas,⁴ Jörg Reinders,⁴ Stefan Hoehme,⁷ Abdel-latif Seddek,⁵ Steven Dooley,⁸ Verena Keitel,⁹ Patricio Godoy,⁴ Brigitte Begher-Tibbe,⁴ Christian Trautwein,¹⁰ Christian Rupp,¹¹ Sebastian Mueller,¹² Thomas Longerich,¹³ Jan G. Hengstler ⁴, Julio Saez-Rodriguez ^{1,3} and Ahmed Ghallab^{4,5}

Mouse models are frequently used to study chronic liver diseases (CLDs). To assess their translational relevance, we quantified the similarity of commonly used mouse models to human CLDs based on transcriptome data. Gene-expression data from 372 patients were compared with data from acute and chronic mouse models consisting of 227 mice, and additionally to nine published gene sets of chronic mouse models. Genes consistently altered in humans and mice were mapped to liver cell types based on single-cell RNA-sequencing data and validated by immunostaining. Considering the top differentially expressed genes, the similarity between humans and mice varied among the mouse models and depended on the period of damage induction. The highest recall (0.4) and precision (0.33) were observed for the model with 12-months damage induction by CCl₄ and by a Western diet, respectively. Genes consistently up-regulated between the chronic CCl₄ model and human CLDs were enriched in inflammatory and developmental processes, and mostly mapped to cholangiocytes, macrophages, and endothelial and mesenchymal cells. Down-regulated genes were enriched in metabolic processes and mapped to hepatocytes. Immunostaining confirmed the regulation of selected genes and their cell type specificity. Genes that were up-regulated in both acute and chronic models showed higher recall and precision with respect to human CLDs than exclusively acute or chronic genes. **Conclusion:** Similarly regulated genes in human and mouse CLDs were identified. Despite major interspecies differences, mouse models detected 40% of the genes significantly altered in human CLD. The translational relevance of individual genes can be assessed at <https://saezlab.shinyapps.io/liverdiseaseatlas/>. (*Hepatology Communications* 2022;6:161-177).

The prevalence of chronic liver diseases (CLDs) has increased during the last decades.⁽¹⁾ Mouse models are frequently used to study the pathophysiology of liver diseases, identify therapeutic targets, and test drug candidates. However, the use of mice in translational research has been criticized due

to large interspecies differences.⁽²⁾ A previous comparison of gene expression in mouse models of non-alcoholic fatty liver disease (NAFLD) and liver tissue from patients reported large interspecies differences, with very little overlap of expression changes in mice and humans.⁽³⁾ This raises the question of whether

Abbreviations: AKR1B10, aldo-keto reductase family 1 member B10; APAP, acetaminophen; ALD, alcohol-associated liver disease; BDL, bile duct ligation; CLD, chronic liver disease; ECM, extracellular matrix; FDR, false discovery rate; GEO, gene expression omnibus; GO, gene ontology; HCV, hepatitis C virus; HE, hematoxylin and eosin; HNF, hepatocyte nuclear factor; logFC, log-fold change; LPS, lipopolysaccharide; LTBP2, latent transforming growth factor beta binding protein 2; MAPK, mitogen-activated protein kinase; NAFLD, nonalcoholic fatty liver disease; NASH, nonalcoholic steatohepatitis; NF-κB, nuclear factor kappa B; PBC, primary biliary cirrhosis; PCA, principal component analysis; PSC, primary sclerosing cholangitis; scRNA-seq, single-cell RNA-sequencing; TGF-β, transforming growth factor β; TNF-α, tumor necrosis factor α; TF, transcription factor; WTD, western-type diet.

Received May 3, 2021; accepted July 9, 2021.

Additional Supporting Information may be found at onlinelibrary.wiley.com/doi/10.1002/hep4.1797/suppinfo.

Supported by LiSyM (031L0045, 031L0049, and 031L0052), TransQST (116030), and EU-ToxRisk (681002).

*These authors contributed equally to this work.

© 2021 The Authors. *Hepatology Communications* published by Wiley Periodicals LLC on behalf of American Association for the Study of Liver Diseases. This is an open access article under the terms of the Creative Commons Attribution-NonCommercial-NoDerivs License, which permits use and distribution in any medium, provided the original work is properly cited, the use is non-commercial and no modifications or adaptations are made.

experiments with mice allow meaningful conclusions to be drawn about the pathophysiology of CLDs in humans. To address this, we here revisited gene-expression changes in mouse models of liver damage and compared them with the human situation.

Previous comparisons of mice and humans were limited by the duration mice were exposed to damaging agents, and typically relied on exposure periods of only a few months or even weeks.^(3,4) This may appear adequate, as extrapolating from the relative lifespans of humans and mice, a 1-year old mouse is comparable to a 40-year old human. However, it remains unknown whether such extrapolation is justified (i.e., whether pathogenesis indeed progresses faster in mice or whether similar periods of damage induction are required to induce comparable phenotypes). To address this question, we analyzed RNA-sequencing data of mice treated with CCl₄ for up to 1 year and compared it to a current collection of human CLD expression data. In addition, we also characterized gene-expression alterations in mice with chronic liver damage in relation to acute injury. This was motivated by a recent study demonstrating that specific expression changes observed in both chronic and acute mouse models are similar to those

observed in human CLD.⁽⁴⁾ Mouse livers responded to acute injury by a concomitant up-regulation of inflammation and down-regulation of metabolism-associated gene regulatory networks that both were orchestrated by the same upstream regulators. A similar response was also observed in a chronic mouse model and was even conserved in human CLDs.⁽⁴⁾ Differentiating between genes exclusively altered in chronic insults and those altered following both chronic and acute damage may be important with respect to defining therapeutic windows. If a gene that is exclusively altered following chronic damage is relevant for disease progression, it should only be therapeutically targeted in advanced stages, when its expression increases; in contrast, genes that are altered in both the chronic and acute setting may be antagonized earlier during the course of the disease.

The present study confirmed the previously reported large interspecies differences, but also revealed substantial sets of genes that respond similarly in both species. The categories of genes exclusively altered after acute or chronic injury compared with those conserved in both damage scenarios differed in their similarity to human CLD, and the similarity to human CLD increased when mice were exposed for longer

View this article online at wileyonlinelibrary.com.

DOI 10.1002/hep4.1797

Potential conflict of interest: Dr. Godoy owns stock in and is employed by Hoffman-La Roche. Dr. Keitel is on the speakers' bureau for AbbVie, Albiro, and Falk. Dr. Saez-Rodriguez consults for Traverre. He received grants for GSK and Sanofi.

ARTICLE INFORMATION:

From the ¹Institute of Computational Biomedicine, Faculty of Medicine, Heidelberg University, Heidelberg, Germany; ²Faculty of Biosciences, Heidelberg University, Heidelberg, Germany; ³Joint Research Centre for Computational Biomedicine, Faculty of Medicine, RWTH Aachen University, Aachen, Germany; ⁴Systems Toxicology, Leibniz Research Centre for Working Environment and Human Factors at the Technical University Dortmund, Dortmund, Germany; ⁵Department of Forensic Medicine and Toxicology, Faculty of Veterinary Medicine, South Valley University, Qena, Egypt; ⁶Dr. Margarete Fischer-Bosch Institute of Clinical Pharmacology, Stuttgart, Germany; ⁷Institute for Computer Science & Saxonian Incubator for Clinical Research, University of Leipzig, Leipzig, Germany; ⁸Department of Medicine II, Medical Faculty Mannheim, Heidelberg University, Mannheim, Germany; ⁹Clinic for Gastroenterology, Hepatology and Infectious Diseases, University Hospital Düsseldorf, Medical Faculty at Heinrich-Heine-University, Düsseldorf, Germany; ¹⁰Department of Medicine III, University Hospital RWTH Aachen, Aachen, Germany; ¹¹Internal Medicine IV, University Hospital Heidelberg, Heidelberg, Germany; ¹²Salem Medical Center and Center for Alcohol Research, University of Heidelberg, Heidelberg, Germany; ¹³Translational Gastrointestinal Pathology, Institute of Pathology, University Hospital Heidelberg, Heidelberg, Germany.

ADDRESS CORRESPONDENCE AND REPRINT REQUESTS TO:

Jan G. Hengstler, M.D. and Ahmed Ghallab, Dr. med. vet.
Systems Toxicology, Leibniz Research Centre for Working
Environment and Human Factors at the Technical University
Dortmund
Dortmund, Germany
E-mail: hengstler@ifado.de, ghallab@ifado.de
Tel.: 0049 231 1084 348, 0049 231 1084 356

or
Julio Saez-Rodriguez, Ph.D.
Institute of Computational Biomedicine, Heidelberg University,
Faculty of Medicine
Heidelberg, Germany
E-mail: pub.saez@uni-heidelberg.de
Tel.: 0049 622 15451210

periods of up to 1 year. These findings were compiled into a data resource linking expression profile alterations of individual genes in CLDs, their differential regulation in mice and humans, and categorization into acute, chronic, or conserved response sets. This resource is accessible through an online application to facilitate the intuitive exploration of the role of genes in human and mice CLD.

Materials and Methods

MOUSE MODELS AND HUMAN DATA SETS

A description of the mouse and human tissues and experimental procedures is available in the Supporting Information. The present analysis included transcriptome data from seven mouse models (one with chronic and six with acute liver damage) consisting of 227 mice (Table 1; Supporting Fig. S1A) and five studies of human CLD with a total of 372 patients (Table 1; Supporting Fig. S1B). The analyzed data sets were either generated in-house (all mouse models except tunicamycin) or downloaded from public sources (acute tunicamycin model and all human data sets). Additionally, we analyzed nine published sets of differentially expressed genes of CLD mouse models, for which the corresponding raw data were not available.⁽³⁾ Biopsies from patients with primary

sclerosing cholangitis (PSC) and alcohol-associated liver disease were used for validation by immunostaining (Supporting Table S1).

BIOINFORMATICS

A comprehensive description of the bioinformatics methods including the processing and analysis of transcriptomic data is given in the Supporting Information. Briefly, time-series gene-expression data were clustered with the software program STEM (short time-series expression miner). The similarity or overlap between two gene sets was summarized either as Jaccard Index or Overlap Coefficient. To test whether the differentially expressed genes of a specific study are consistently regulated in an independent study, gene-set enrichment analysis was performed. Differential genes across all the signatures derived from the chronic or acute mouse experiments were classified as exclusively chronic, exclusively acute, or commonly regulated in chronic and acute and for each of these three gene sets, a custom metric was computed to rank each gene. Functional characterization of transcriptomic data was performed by Gene Ontology (GO), DoRothEA's regulons^(14,15) and PROGENY's pathway analysis.^(15,16) Identification of consistently deregulated genes in patients and the chronic CCl₄ mouse model was based on leading-edge genes derived from at least three human studies per chronic time point.

TABLE 1. MOUSE MODELS AND PATIENT COHORTS WITH GENOME-WIDE EXPRESSION DATA OF LIVER TISSUE

Organism	Damage	Treatment	N*	Accession ID	Reference
Mouse	Chronic [†]	CCl ₄ (up to 12 months)	36	GSE167216	Ghallab et al. 2019 ⁽⁵⁾ and present study
Mouse	Acute	APAP (up to 16 days)	49	GSE167032	Present study
Mouse	Acute [†]	CCl ₄ (up to 16 days)	46	GSE167033	Campos et al. 2020 ⁽⁴⁾ and present study
Mouse	Acute	Partial hepatectomy (up to 3 months)	52	GSE167034	Present study
Mouse	Acute ^{†,‡}	BDL (up to 3 weeks)	29	GSE166867	Ghallab et al. 2019 ⁽⁶⁾ and present study
Mouse	Acute [†]	LPS (24 hours)	8	GSE166488	Godoy et al 2016 ⁽⁷⁾
Mouse	Acute	Tunicamycin (6 hours)	7	GSE29929	Teske et al 2011 ⁽⁸⁾
Human	Chronic	Mild vs. advanced NAFLD	72	GSE49541	Diehl et al. 2014 ⁽⁹⁾
Human	Chronic	Full spectrum of NAFLD	78	GSE130970	Hoang et al. 2019 ⁽¹⁰⁾
Human	Chronic	NAFLD and NASH	46	GSE48452	Hampe et al. 2013 ⁽¹¹⁾
Human	Chronic	NASH, NAFLD, PBC, and PSC	109	GSE61260	Hampe et al. 2014 ⁽¹²⁾
Human	Chronic	HCV and NAFLD	67	E-MTAB-6863	Ramnath et al. 2018 ⁽¹³⁾

*Sample size.

[†]Data set generated by our group, in which the raw data is made publicly available for the first time.

[‡]Only the 24-hour time point was analyzed to focus on the acute damage after BDL.

Results

CHRONIC LIVER DAMAGE IN MICE

To study genome-wide expression changes time-dependently in a long-term mouse liver damage model, we administered the hepatotoxic compound CCl_4 twice weekly for up to 1 year. Six animals per group were analyzed by RNA-sequencing after 2, 6, and 12 months; liver tissue was sampled 6 days after the last CCl_4 dose to avoid capturing the acute expression response (Fig. 1A). Histological analyses showed progressive fibrosis, particularly between months 6 and 12, accompanied by increased transaminase enzyme activities in blood (Fig. 1B,C). Principal component analysis (PCA) revealed that mice from the individual treatment groups clustered together; chronic CCl_4 intoxication led to a shift inversely along with principal component 1 (PC1), while the solvent oil caused a shift along PC2 (Supporting Fig. S2A). The number of differentially expressed genes particularly increased between months 6 and 12 (Supporting Fig. S2B,C; Supporting Table S2). Overlapping genes with the highest up-regulated fold changes in all three exposure periods include the extracellular matrix (ECM) protein Col28a1, two sulfotransferase isoforms (Sult2a1 and 2a2), the basement membrane glycoprotein Tinag, and the positive regulator of PP1 phosphatase Ppp1r42, which plays a role in centrosome separation (Fig. 1D,E). Those among the most significantly down-regulated are three members of the lipocalin family (Mup12, Mup15, and Mup19), and the DBH-like monooxygenase protein 1, Moxd1. Time-dependent clustering resulted in seven clusters: four with up, two with down, and one with initially up and later down-regulated genes (Fig. 1F; Supporting Table S3). Up-regulated clusters were enriched in inflammation and proliferation-associated genes, with *Lyl1* and *Maf* as the most overrepresented transcription factors, and tumor necrosis factor α (TNF- α) as well as nuclear factor kappa B (NF- κ B) as the most overrepresented pathways. The dominant GO terms of the down-regulated clusters were all metabolism-associated, with hepatocyte nuclear factor (HNF)1 α and HNF4 α as the most significantly overrepresented transcription factors (TFs). The initially up-regulated and later down-regulated cluster were associated with ECM-related processes.

In summary, transcriptomics corroborates the results of the histological analyses, showing (1) progressive inflammation and fibrosis with a relatively mild phenotype until month 6, and (2) massive progression between months 6 and 12.

ACUTE LIVER DAMAGE IN MICE

We first analyzed similarities and differences of these described chronic liver damage models to acutely injured mouse livers to be able to compare both with chronic liver damage in humans afterward. For this purpose, we initially studied six acute injury models induced by different damage types. The acute acetaminophen (APAP) model is presented as an example in Fig. 2, with corresponding summaries of the other models in Supporting Figs. S4-S9.

To induce acute liver injury, mice were treated once with a hepatotoxic dose of 300 mg/kg body weight APAP, and the transcriptome was profiled at nine time points after injection, spanning from 1 hour to 16 days (Fig. 2A). Histological analyses showed pericentral hepatocyte death on day 1 with almost complete regeneration until day 8, without the formation of fibrosis (Fig. 2B). Infiltration of CD45-positive immune cells was observed between days 1 and 4, and clinical chemistry analysis showed a transient increase in liver enzymes (Fig. 2C). Thus, the histological alterations are in accordance with previous studies of APAP intoxication in mice.⁽¹⁷⁾ In the PCA space, differences to the controls were largest between 12 hours and day 2 and subsequently returned toward the control levels (Fig. 2D). The same trend was also reflected in the number of differentially expressed genes (Fig. 2E; Supporting Fig. S3A,B). Clustering of gene-expression trajectories resulted in seven clusters, three with up-regulated and four with down-regulated genes (Fig. 2F; Supporting Table S3). Up-regulated clusters were enriched in stress response, migration, and proliferation-associated genes with *Atf3*, *Sp1*, and *E2f4* as enriched TFs, and transforming growth factor β (TGF- β) as the most enriched pathway. Genes belonging to the down-regulated clusters were predominantly metabolism-associated with HNF4 α and *Cebpa* as the most significantly enriched TFs.

A common feature among the studies with acute time-series is that the maximal number of deregulated genes was reached at 24 or 48 hours after the intervention and returned almost completely to control

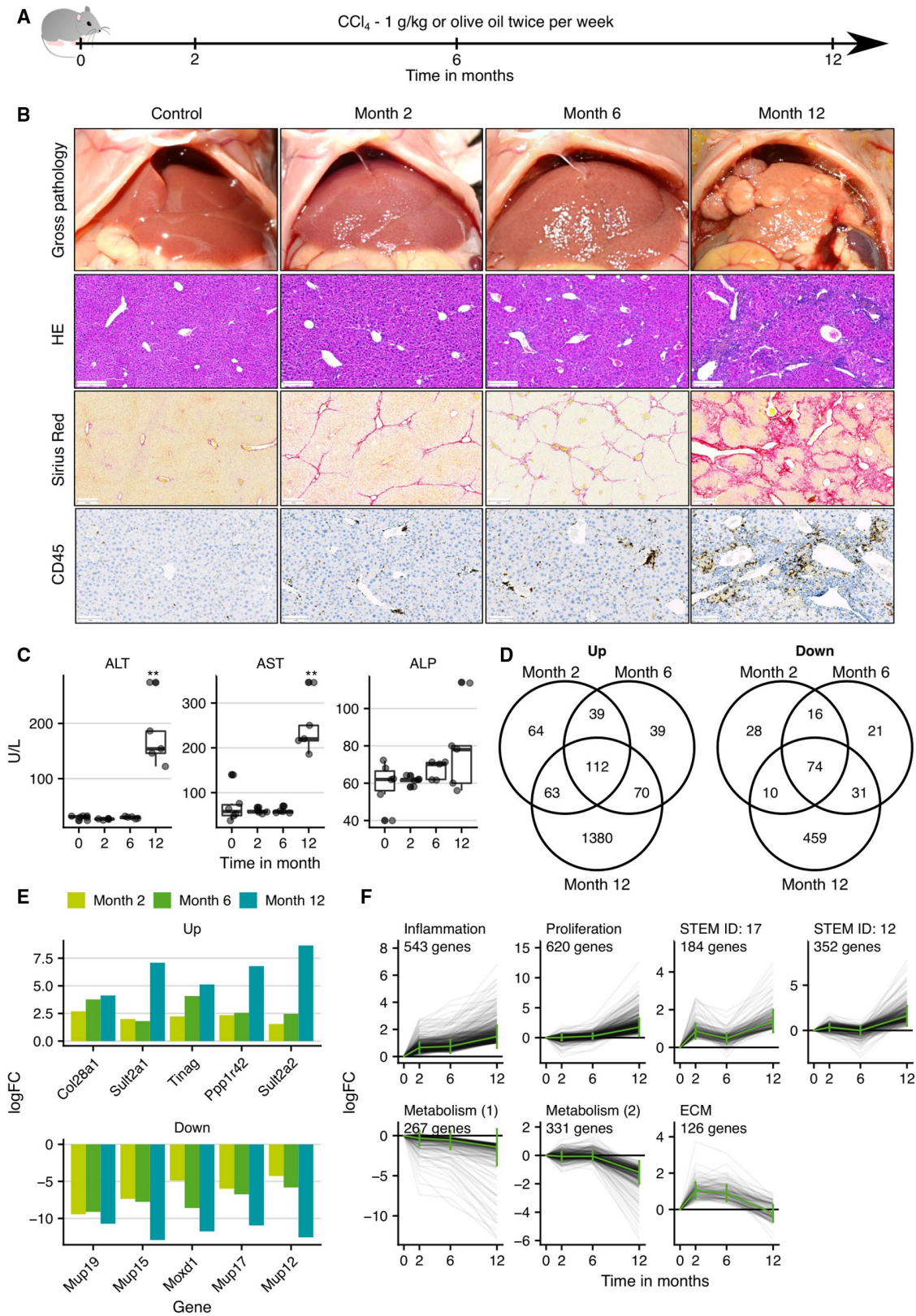


FIG. 1. Gene-expression changes in the CCl₄ mouse model of CLD. (A) Experimental design. Six mice were analyzed in each treatment group. (B) Histological analyses with hematoxylin and eosin (HE) staining, visualization of fibrosis by sirius red, and infiltration of immune cells by CD45; scale bars: 200 μ m (HE and sirius red) and 100 μ m (CD45). (C) Clinical chemistry of alanine transaminase, aspartate transaminase, and alkaline phosphatase activities in plasma. (D) Overlaps of up-regulated and down-regulated genes. (E) Genes in the overlap of the three exposure periods with the highest fold changes. (F) Time-resolved clustering of deregulated genes with the dominant GO terms or the default profile names (STEM ID), if no significantly overrepresented GO term was obtained. **FDR < 0.01. Abbreviations: ALP, alkaline phosphatase; ALT, alanine transaminase; AST, aspartate transaminase.

levels within 16 days (Supporting Figs. S4D and S6D). An exception was bile duct ligation (BDL), in which expression changes persisted due to the irreversible obstruction of the bile duct (Supporting Fig. S8D). To investigate the consistency of the gene-expression profiles across the six acute mouse models, we compared the similarity of the top 500 differentially expressed genes using the time point with the strongest deregulated expression profile (Supporting Fig. S10) and the 24-hour time point for BDL.

Globally, we found a low gene overlap across the six acute models (mean Jaccard Index of 0.058; Fig. 3A), with the highest similarity between APAP and CCl₄ (Jaccard Index of 0.157) and the lowest between lipopolysaccharide (LPS) and tunicamycin (Jaccard Index of 0.012). This pairwise comparison revealed that each treatment yields a distinctive set of top differentially expressed genes. Next, we tested whether the direction of regulation of the top differentially expressed genes is conserved across the six acute mouse models. A pairwise enrichment of the top 500 up-regulated and down-regulated genes in the acute damage signatures showed that the different sets of up-regulated genes were coordinately up-regulated in all other acute damage signatures (Fig. 3B). The same applied to the sets of down-regulated genes. These systematic comparisons demonstrated that although the top differentially expressed genes were distinct, the direction of gene regulation was consistent among the models, suggesting that it was adequate to integrate all of the available acute scenarios for further comparison with the chronic situation.

EXCLUSIVELY AND COMMONLY REGULATED GENES OF CHRONIC AND ACUTE LIVER DAMAGE IN MICE

To identify sets of exclusively chronic, exclusively acute, and common acute and chronic genes, we next integrated and analyzed all available acute and chronic time points. The unified differentially expressed genes

of the acute studies and also the chronic CCl₄ mouse model showed consistent up-regulation or down-regulation across the individual signatures, respectively (Supporting Fig. S11). In total, we identified 834 exclusive chronic, 2,777 exclusive acute, and 586 common genes (Supporting Table S4). We functionally characterized these gene sets by overrepresentation analysis. As gene-set resources, we used DoRotheA's transcription factor regulons,^(14,15) PROGENY's pathway footprints,^(15,16) and GO terms of biological processes. Because unifying all differentially expressed genes can lead to many false-positive genes, we finally identified the top 100 most relevant genes in each category by ranking the genes based on their expression in the chronic and selected acute signatures.

In the top 100 exclusive chronic genes, 97 were up-regulated and only 3 were down-regulated (Fig. 3C). We found the target genes from the TFs Hif1 α and Klf, as well as the footprint genes from the TGF- β pathway enriched in the set of upregulated exclusive chronic genes (Fig. 3D). Text analysis of overrepresented GO terms revealed that most processes were associated with development and morphogenesis (Fig. 3D). By manual classification, we found 38 GO terms related to "development and morphogenesis" and 24 GO terms related to "migration," with the latter being more pronounced among the most significantly overrepresented GO terms. Functional characterization of the down-regulated exclusive chronic genes highlighted the TFs Stat3, Sox2, and Hoxb13. Pathways, as well as GO terms, however, did not result in any significant associations.

For the top 100 exclusive acute genes (Supporting Fig. S12A), the up-regulated genes were associated with the TFs Myc and Trp53, and the pathways mitogen-activated protein kinase (MAPK), epidermal growth factor receptor (EGFR), and TNF- α (Supporting Fig. S12B,C). GO terms were dominated by metabolic processes; however, we also identified a cluster of endoplasmic reticulum stress-related processes among the most significant GO terms

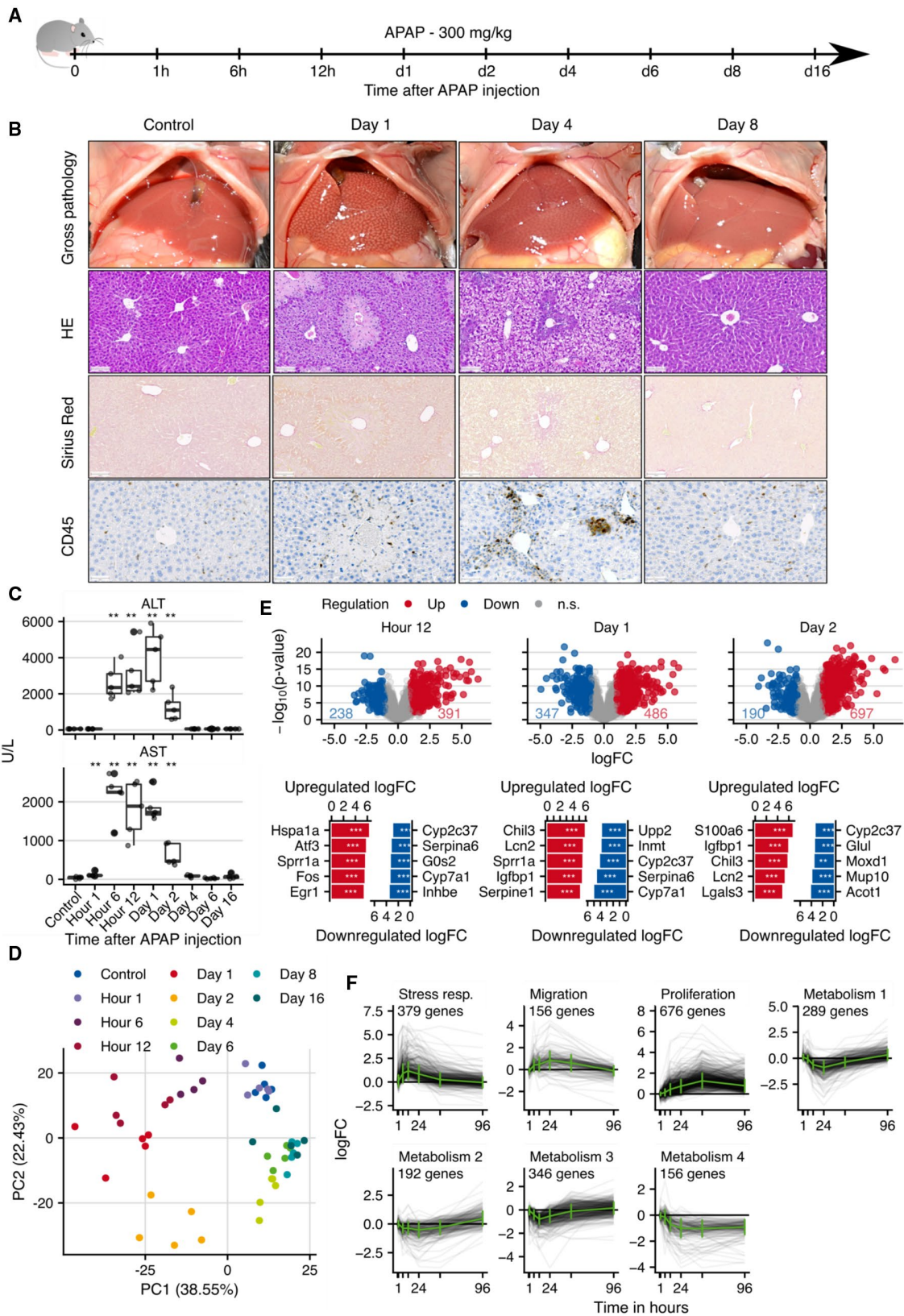


FIG. 2. Gene-expression changes in a mouse model of acute liver damage induced by administration of 300 mg/kg body weight APAP. (A) Experimental design. Five mice were analyzed in each treatment group. (B) Histological analyses with HE staining, lack of fibrosis visualized by sirius red, and infiltration of immune cells by CD45 immunostaining; scale bars: 100 μ m (HE and sirius red) and 50 μ m (CD45). (C) Clinical chemistry of alanine transaminase and aspartate transaminase activity in plasma. (D) PCA of global expression changes. (E) Volcano plots of gene-expression changes and genes with highest logFCs at 12 hours, days 1 and 2 after APAP administration. (F) Time-resolved clustering of deregulated genes. **FDR < 0.01 and ***FDR < 0.001. Abbreviations: ALT, alanine transaminase; AST, aspartate transaminase.

(Supporting Fig. S12D). Down-regulated genes were associated with the TFs *Hnf4a*, *Ubt1*, and *Zfp263* and the pathways androgen-signaling, estrogen-signaling, EGFR-signaling, and MAPK-signaling (Supporting Fig. S12E,F). GO terms were also almost exclusively related to metabolic processes (Supporting Fig. S12G).

Out of the top 100 common genes, 53 were consistently up-regulated and 47 down-regulated (Fig. 3E). Functional analysis of the up-regulated genes identified the TF *Klf5* and the pathways NF- κ B and TNF- α as relevant (Fig. 3F). Among the overrepresented GO terms, the term cell cycle had the highest frequency (Fig. 3F). In agreement, we identified a cluster of 37 most significant GO terms that corresponds to the biological process of proliferation. Down-regulated genes were associated with the TFs *Hnf4a* and *Nr4a1* (Supporting Fig. S13A), and biological processes were dominated by metabolic GO terms (Supporting Fig. S13B). Thus, the integration of chronic and acute mouse data unveiled genes that are deregulated in both damage models, and can be differentiated from gene sets exclusively deregulated in either acute or chronic liver damage.

CONSISTENTLY REGULATED GENE SETS IN HUMANS AND MICE

Finally, we performed a cross-species analysis to study whether genes exist that are consistently altered in patients with CLD and (1) the here-described chronic CCl₄ mouse model, (2) nine previously published CLD mouse models for which sets of differentially expressed genes were available,⁽³⁾ and (3) sets of exclusively and commonly regulated genes of chronic and acute mouse models as defined previously. For this purpose, we collected genome-wide gene-expression data from five publicly available patient cohorts with a total of 372 patients and five etiologies.⁽⁹⁻¹³⁾ Similar to the acute mouse models, we first analyzed interstudy consistency among patient cohorts, comparing the

similarity of the top 500 differentially expressed genes from each signature (Supporting Table S5). Differential genes obtained from studies originating from the same groups of authors showed a higher degree of similarity (Supporting Fig. S14A). The highest similarity of two independent sets of differentially expressed genes was observed between NAFLD⁽⁹⁾ and hepatitis C virus (HCV)⁽¹³⁾ (Jaccard Index of 0.154). However, the similarity of the top differentially expressed genes in humans appeared to be low. Nevertheless, pairwise enrichment of the top 500 up-regulated and down-regulated genes demonstrated a very high consistency with respect to the direction of regulation (Fig. 4A). The direction of regulation of genes from the patients with PSC, PBC,⁽¹²⁾ and NAFLD⁽¹¹⁾ was not conserved in other liver diseases. However, all other pairwise comparisons yielded consistent results. Moreover, basal expression levels of patients with NAFLD stage 0 and of untreated mice were analyzed showing a high degree of correlation (Supporting Fig. S14B).

A cross-species enrichment analysis between our chronic CCl₄ model and the set of human data was then performed, enriching the top 500 up-regulated and down-regulated genes from each human signature in the three signatures from the individual time points of the chronic CCl₄ experiment in mice. We found a high degree of accordance, in which almost all human gene sets, with the exception of the PBC gene set, were significantly and consistently enriched at any time point of the chronic CCl₄ mouse signatures (Fig. 4B). To identify genes consistently deregulated in humans and mice, we extracted the leading-edge genes from these conducted enrichment analyses with significant and consistent results in terms of the direction of regulation. Subsequently, we kept only those leading-edge genes that were identified in at least three human studies per time point in the chronic mouse model. This resulted in 126 consistently up-regulated and 102 consistently down-regulated genes, of which 45 (up) and 23 (down) genes were shared among all three chronic time points (Fig. 4C; Supporting Table S6).

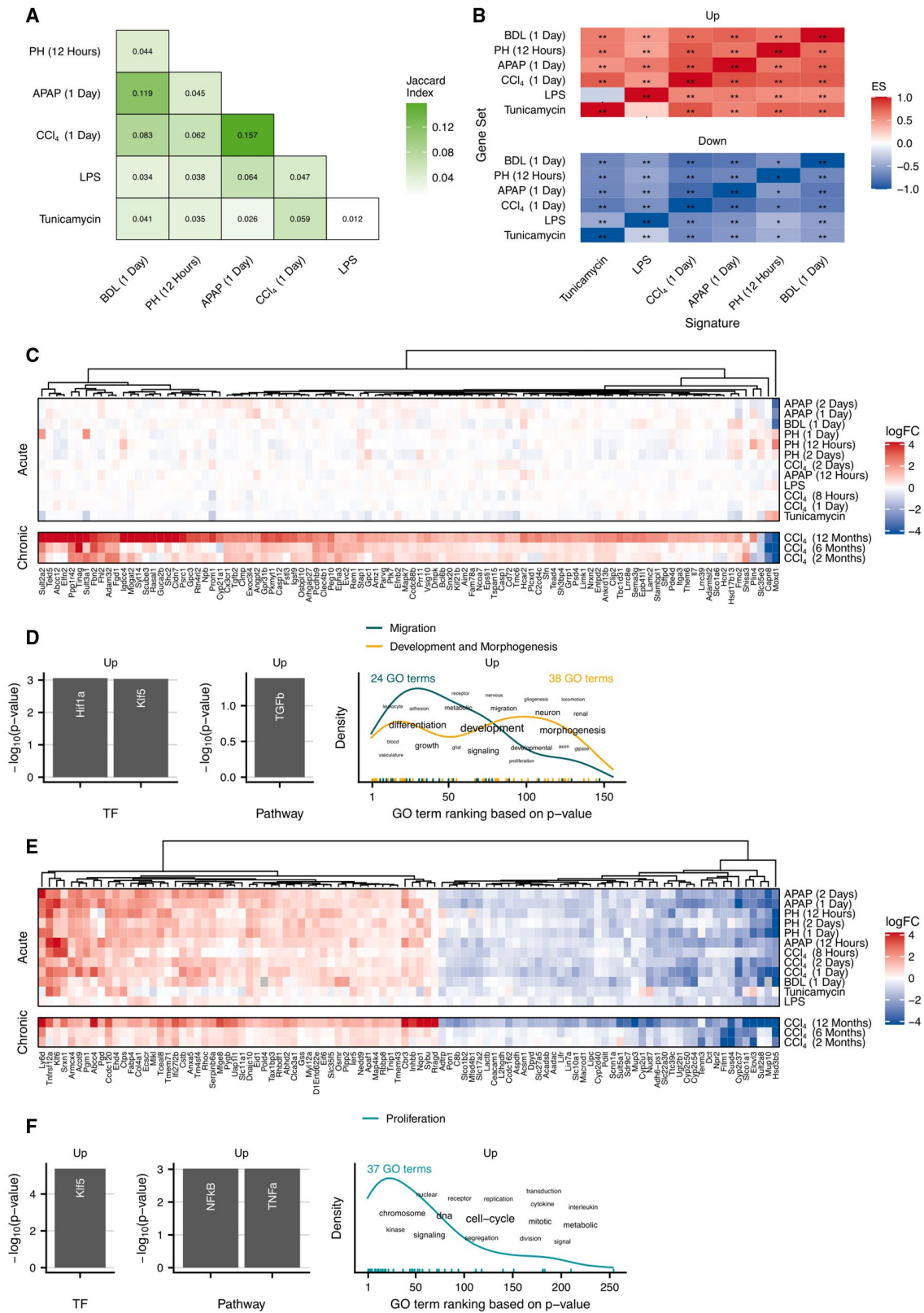


FIG. 3. Comparison of gene-expression changes in acute and chronic mouse models. (A) Analysis of the similarity of the acute data sets. As a measure of similarity, the Jaccard index was calculated at the indicated time periods after the acute challenge. (B) Pairwise enrichment analysis of the top 500 up-regulated and down-regulated genes (enrichment score). (C) Heatmap of genes exclusively deregulated in the chronic mouse model. (D) Overrepresented transcription factors, identified by DoRothEA, pathways obtained by PROGENy, and GO terms in the up-regulated exclusive chronic genes. (E) Heatmap of genes up-commonly deregulated in the chronic and acute mouse models. (F) DoRothEA, PROGENy, and GO overrepresentation of the genes up-regulated in the acute and chronic mouse models. FDR < 0.1, *FDR < 0.05, and **FDR < 0.01. Abbreviations: ES, enrichment score; PH, partial hepatectomy.

To map the 228 commonly altered genes to individual cell types of the liver, we integrated single-cell RNA-sequencing (scRNA-seq) data with our existing bulk data. For this purpose, we re-analyzed a publicly available scRNA-seq data set of patients with cirrhosis and healthy controls annotated with different cell types.⁽¹⁸⁾ Differentially expressed genes between patients with cirrhosis and healthy patients were identified for each cell type individually (false discovery rate [FDR] ≤ 0.05 & log-fold change |logFC| ≥ 0.25). The resulting cell type-associated sets of differential genes overlapped with 50 of these described 228 genes that are consistently regulated in humans and mice (Supporting Table S6). From the total 228 consistently deregulated genes, we identified the top 100 genes with respect to the highest average logFC across all human and mouse bulk signatures (Fig. 4D). Of those 100 genes, 79 were up-regulated and 21 were down-regulated, and 31 were mapped to a specific cell type. Overall, the direction of regulation was consistent between bulk and scRNA-seq data.

A functional characterization was performed separately for all up-regulated and down-regulated genes. The up-regulated genes were significantly associated with the pathways TGF-β and TFN-α, and the TFs SP1, RELA, and NF-κB1 (Fig. 4E). Biological processes related to migration and development and morphogenesis functionally characterize the up-regulated genes (Fig. 4E). The down-regulated genes were dominated by metabolic processes, including the androgen signaling pathway (Supporting Fig. S15A,B). Remarkably, we found that the up-regulated genes frequently mapped to cholangiocytes, endothelial cells, mesenchymal cells, and macrophages, whereas the down-regulated genes mapped mostly to hepatocytes. Mapping the consistently deregulated genes back to the 12-month signature of the chronic CCl₄ mouse model revealed that the logFCs for up-regulated genes are generally higher compared with the down-regulated genes (Fig. 4F). Furthermore, genes consistently regulated between humans and

mice did not show particularly low *P* values or high fold changes, compared with all deregulated genes following CCl₄ treatment.

The consistent regulation in humans and mice, as well as the cell-type specificity of gene expression, was confirmed at the protein level, using commercially available antibodies against three of the consistently up-regulated genes, latent transforming growth factor beta binding protein 2 (LTBP2), annexin V (ANXA5), and aldo-keto reductase family 1 member B10 (AKR1B10). A strong increase in the ECM protein LTBP2 occurred after 12 months of CCl₄ treatment in mice, and was expressed in the fibrotic tissue but not in the hepatocytes (Fig. 5A). For analysis of the human situation, we used independent biopsies of patients with PSC. Because CCl₄ induces pericentral necrosis in mice and a similar zonation is known for alcohol-associated liver disease (ALD),⁽¹⁹⁾ we additionally tested biopsies of patients with ALD. Similar to mice, LTBP2 was expressed in the fibrotic streets of PSC (Fig. 5B) and patients with ALD (Fig. 5C), and the staining intensity increased with fibrosis stage. Expression in fibrotic tissue also confirmed the results of the scRNA-seq analysis that identified a mesenchymal cell-type preference of LTBP2. Immunostaining of the aldo-keto reductase AKR1B10 and of ANXA5 also showed similar up-regulation in mouse and human CLD (Supporting Fig. S16).

Next, we placed the deregulated genes identified in the present chronic CCl₄ study into the context of previously published chronic mouse models and compared them with human CLDs. In contrast to the human data, for which the raw data were made publicly available, only lists of the differentially expressed genes were available for the previously published chronic mouse models. Accordingly, our analysis was limited to the comparison of the reported differentially expressed genes. The 12-month chronic CCl₄ model resulted in a much higher number of differentially expressed genes than all other previously published mouse models, considering the same cutoff that

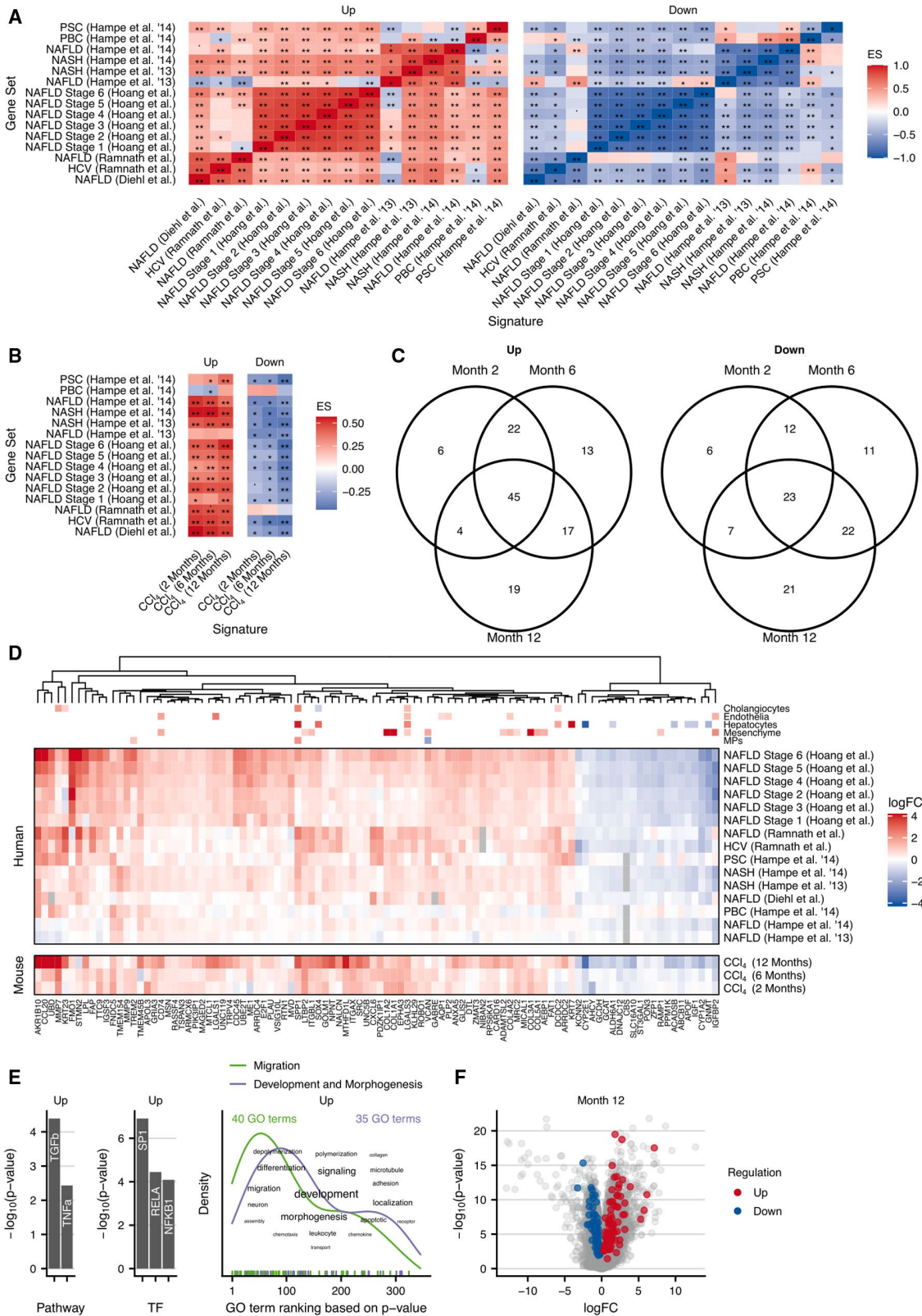


FIG. 4. Human studies of liver disease and their similarities to the chronic CCl₄ mouse model. (A) Pairwise enrichment analysis of the top 500 up-regulated or down-regulated genes of the human studies (enrichment score). (B) Similarity between the human studies and the chronic CCl₄ mouse model by pairwise enrichment analysis of the 500 top up-regulated and down-regulated genes. (C) Overlaps of up-regulated and down-regulated genes in the chronic mouse model after 2, 6, and 12 months of CCl₄ administration that are consistently regulated in the human studies. (D) Heatmap of the top 100 genes consistently regulated in the human studies and in the chronic CCl₄ mouse model. (E) Characterization of the consistently deregulated genes in humans and mice by analysis of enriched pathways, transcription factors, and GO terms. (F) Volcano plot of genes consistently deregulated in mouse and human (red and blue symbols) projected onto all genes deregulated in the chronic mouse model with CCl₄ (gray symbols). FDR < 0.1, *FDR < 0.05, and **FDR < 0.01. Abbreviations: ES, enrichment score; MP, macrophage.

was applied for the published mouse models (2,721 up-regulated and 1,437 down-regulated genes; FDR ≤ 0.05 & |logFC| ≥ log₂(1.5); Supporting Fig. S17A). In contrast, a model of the 18-week high-fat diet feeding yielded only 16 up-regulated and 19 down-regulated genes, when applying the same cutoffs.⁽³⁾ Similarity analysis of the differentially expressed genes between the chronic mouse models and the patient cohorts showed that the 12-month time point of the chronic CCl₄ model was more similar to human data than all other models (mean overlap coefficient of 0.37; Supporting Fig. S17B). However, this analysis is biased toward the total number of differentially expressed genes.

To study how well mouse models reflect expression changes in human CLD, independently from the total number of differentially expressed genes in mice, we first identified the differentially expressed genes of the same human etiology (NAFLD, nonalcoholic steatohepatitis [NASH], HCV, PSC, and PBC; Supporting Table S5). Most of the differentially expressed genes occurred in a single disease (84.9%), and no single gene was differentially expressed in all etiologies (Fig. 6A). To quantify the similarity between the individual chronic mouse models and the different human disease-specific gene sets, we computed precision and recall metrics. Recall denotes the ratio of altered human genes that are also altered in mice with respect to all altered human genes. Precision denotes the ratio of genes altered in mice that are also altered in humans with respect to all altered mouse genes. In general, precision and recall of the chronic mouse models for the different human disease etiologies were highly variable (Fig. 6B). Precision and recall pairs were highest for NAFLD and lowest for PBC. The 12-month chronic CCl₄ model showed the highest recall among all etiologies. Moreover, recall of 12-month CCl₄ was always higher than that of the 6-month or 2-month damage periods. The Western-type diet

(WTD) model had the highest precision related to the up-regulated genes of NAFLD.

We revisited the exclusively and commonly regulated genes of chronic and acute mouse models (Fig. 3) to study their similarity to human CLD (Fig. 6C). As expected, exclusive acute mouse genes showed the lowest recall and precision with respect to CLD. Remarkably, common genes (deregulated in acute and chronic mouse models) resulted in higher metrics than the exclusive chronic genes for several comparisons, particularly with respect to NAFLD. As a final aspect, we analyzed whether the combination of either ethanol and CCl₄,⁽²⁰⁾ as well as WTD and CCl₄⁽²¹⁾ improved the similarity of expression profiles to human CLD etiologies. In both cases, the combination improved recall for the up-regulated genes, while no systematic influence on precision was observed (Supporting Fig. S18A,B).

GENE BROWSER FOR COMPARISON OF HUMAN AND MOUSE LIVER DISEASE

To facilitate the assessment of the translational relevance of mouse models for specific human liver diseases, we established an open-access gene browser (<https://saezlab.shinyapps.io/liverdiseaseatlas/>). This application provides for any gene of interest mean expression changes in the individual human and mouse studies, categorization into acute, chronic or common response sets, the associated cell type, and whether the gene is consistently altered in mice and humans.

Discussion

Although several preclinical developments have successfully been performed in mouse models,⁽²²⁾ it is

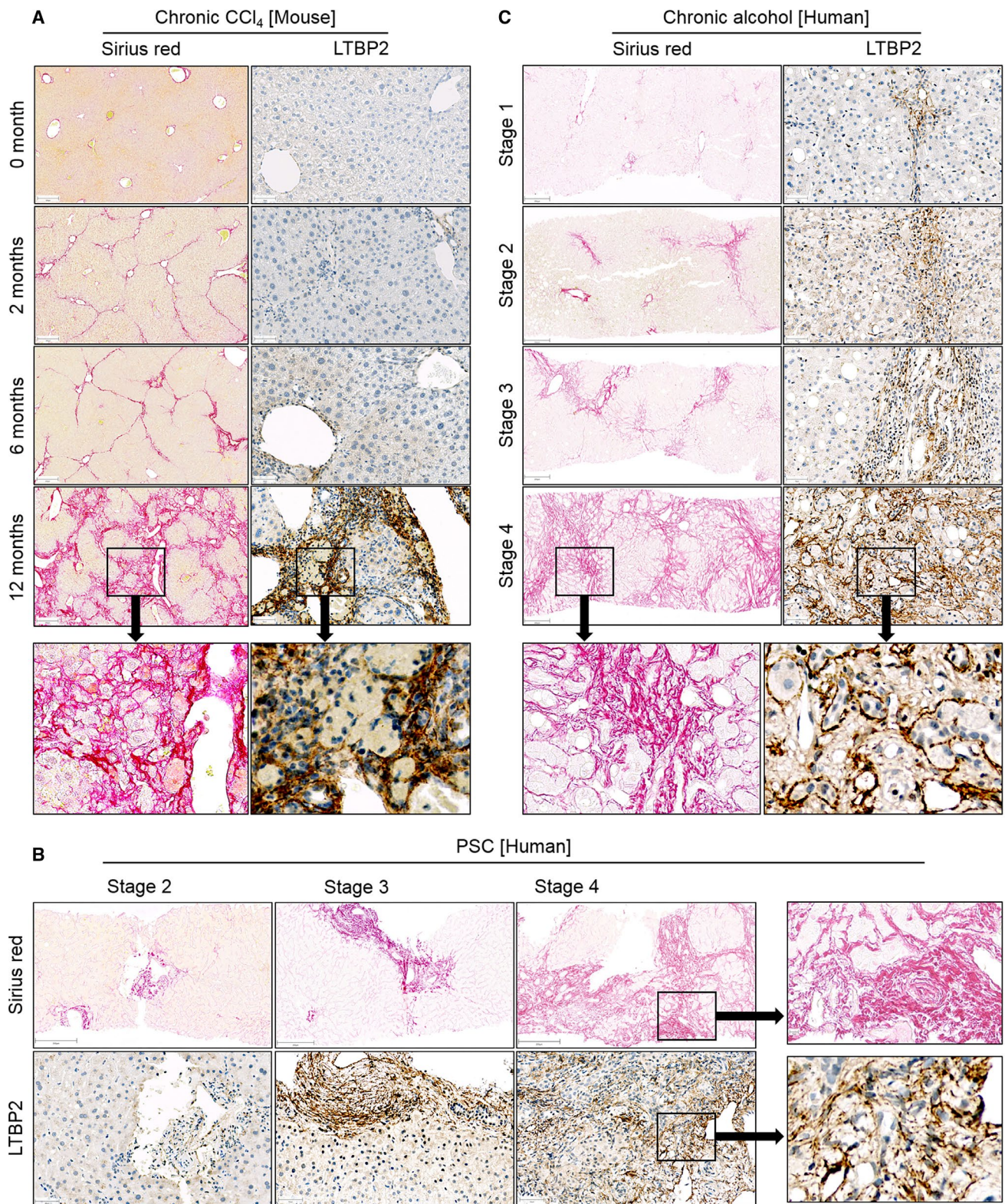


FIG. 5. The ECM protein LTBP2 increases in CLD of mice and humans. (A) Liver tissue of mice at different time periods after CCl₄ treatment. (B) Liver tissue of patients with different stages of PSC. (C) Liver tissue of patients with ALD of different stages. Stainings were performed with sirius red (scale bars: 200 μ m) to visualize fibrosis and with antibodies against LTBP2 (scale bars: 200 μ m) in liver tissue of the same patients.

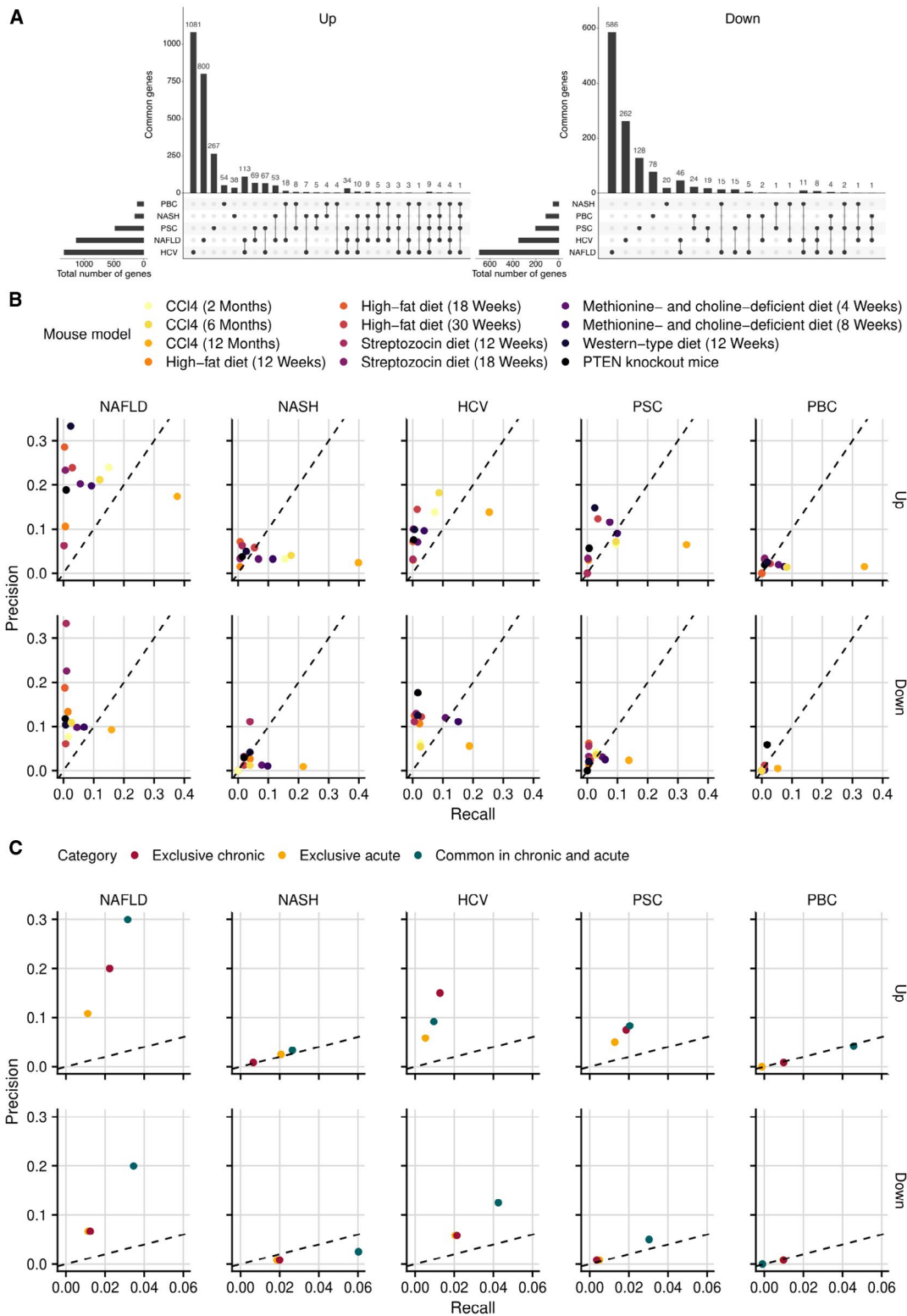


FIG. 6. Recall and precision of 12 individual mouse models with respect to the human liver diseases NAFLD, NASH, HCV, PBC, and PSC. (A) Gene sets that are uniquely or commonly deregulated in individual human diseases. (B) Recall and precision of the individual mouse models with respect to the five human liver diseases. All genes with $FDR \leq 0.05$ & $|\log_2FC| \geq \log_2(1.5)$ were included. (C) Comparison of exclusive chronic, exclusive acute, and common genes in acute and chronic mouse models to human data. To allow a direct comparison, the top 120 genes of each category were included. Abbreviation: PTEN, phosphatase and tensin homolog.

also well-known that large differences exist between human and mouse liver pathophysiology. A previously published comparison of gene-expression changes in liver tissue of patients with NAFLD and NASH to mouse models reported very little overlap.⁽³⁾ Here, we revisited this topic for three reasons. First, the availability of expression data of patients with CLD has increased in the past years. The previous mouse–human comparison from 2016 included genome-wide expression data of 25 patients with NAFLD and 27 with NASH⁽³⁾; however, since then, a much larger genome-wide expression database of human liver diseases is available, but has not yet been systematically evaluated. Here, we have leveraged these data and used 372 genome-wide expression profiles of patients with NAFLD (n = 147), NASH (n = 42), HCV (n = 23), PBC (n = 11), and PSC (n = 14). The remaining 135 profiles were from healthy/control patients. Second, it is currently unclear whether longer exposure periods in chronic mouse models will improve the similarity between mice and human CLD. Third, a recent study suggested that a stress response with up-regulated inflammatory and down-regulated metabolic genes occurs similarly in acute and chronic mouse models and in human CLD. Thus, a comprehensive mouse–human comparison should differentiate among acute, chronic, and common expression responses.⁽⁴⁾

Of all the analyzed chronic studies, the mouse model with 12 months of CCl₄ administration led to the highest recall of genes significantly altered in human liver diseases. Specifically, 38%, 40%, 25%, 34%, and 33% of all significantly up-regulated genes in NAFLD, NASH, HCV, PBC, and PSC, respectively, were also up-regulated in the 12-month CCl₄ mouse model (Fig. 6B). Considering a previous study that reported very little overlap in expression changes between mouse and human,⁽³⁾ our findings represent a remarkably high recall. A critical factor for the relatively large mouse–human overlap is the long exposure period of the mice. It should be considered that the recall of up-regulated genes for human NASH was only 0.16 and 0.18 if the mice were exposed for 2 or 6 months, but increased to about 0.4 after 12 months. Similarly, as for NAFLD and NASH, an increase in recall between 6 and 12 months was obtained for the comparisons of the mouse data with all other human diseases. This demonstrates that the relatively short exposure periods used in previous mouse studies may explain the small overlap of expression changes

between diseased human and mouse livers. Although the recall was generally smaller for the down-regulated than the up-regulated genes, the same basic observations were made with respect to time. In contrast to the high recall, precision was lower for the 12-month CCl₄ mouse model, which suggests that besides a set of genes of human relevance, numerous further expression changes occur in mice that are not observed in humans. Among the 12 mouse models analyzed, the WTD presented with the highest precision (0.33) for human NAFLD. This was not unexpected, considering the similarity in disease etiology. However, the WTD mouse model had a low recall (0.02), which may be due to the relatively short feeding period of only 3 months.⁽³⁾ Assuming that there is a similar time dependency as for the CCl₄ model, further studies with longer WTD feeding periods may improve the concordance. The here established recall and precision metrics to assess the similarity of mouse and human expression profiles was also applied to two published data sets in which WTD and ethanol exposure were combined with low doses of CCl₄, respectively.^(20,21) The combination improved recall but not precision.

From a bioinformatics perspective, overlap analysis of differentially expressed genes may not be the optimal approach to identify a consensus set of genes altered in a specific human CLD and in a mouse model. Instead, we propose enrichment analysis to be superior, as it focuses on the direction of regulation and not the effect size of individual genes.⁽²³⁾ Of note, this approach requires access to raw or processed data. Following the enrichment analysis strategy, a more sophisticated comparison of the chronic CCl₄ mouse model and human studies identified a set of 228 genes with similar regulation in mouse and human CLDs. These genes are enriched in the GO terms' migration, development, and morphogenesis, and several are associated with immune cells and ductular reactions. Based on scRNA-seq, we found that the up-regulated genes mostly mapped to cholangiocytes, macrophages, and endothelial and mesenchymal cells, whereas the down-regulated genes were mostly assigned to hepatocytes. This corresponds to known features of CLDs, in which the number of cholangiocytes increases due to ductular reactions, while macrophages, mesenchymal cells, and endothelial cells are involved in inflammatory processes associated with the identified enriched GO terms among the up-regulated genes, such as

migration and adhesion. In contrast, the metabolism-associated genes in hepatocytes are predominantly down-regulated. Selected genes up-regulated in mouse and human CLDs were further analyzed at the protein level. An interesting example is the ECM protein LTBP2, which is involved in anchoring the latent form of TGF- β in the ECM and plays a role in cell adhesion and tumor promotion.^(24,25) LTBP2 stained negative in normal livers of mice, was weakly positive after 2 and 6 months of CCl₄, and had an intense signal at 12 months. Similarly, human PSC and alcohol-associated liver fibrosis showed positive LTBP2 staining that increased with the stage of fibrosis. It will be interesting to analyze whether up-regulation of LTBP2 is related to TGF- β signaling activity, as the TGF- β pathway was identified as significantly up-regulated. Two further genes identified as commonly up-regulated in human and mouse CLDs, AKR1B10 and ANXA5, had similar changes in gene and protein expression. Although comprehensive validation is still required, these preliminary immunostainings demonstrate that the here identified mouse-human consensus set includes genes that can be validated at the protein level.

To compare exclusively acute, exclusively chronic, and genes altered in both scenarios (common) in mice with human CLD, we generated additional mouse data from acute challenges. Across the different acute challenges induced by chemical and surgical insults, we observed expression alterations in sets of exclusively acute and chronic, as well as common genes. Differentiation of the three categories appeared relevant when compared with human CLD. Exclusively acute genes minimally overlapped with human genes, which is not surprising considering the chronic nature of CLD. The common mouse genes showed the highest similarity with CLD in patients, particularly for NAFLD and NASH. This was surprising, because the damaging agent CCl₄ differs from the hypercaloric and high fat etiology of human NAFLD/NASH. An explanation may be the recently published concept that different types of damage cause similar expression alterations in mouse and human liver with up-regulated inflammatory and down-regulated metabolic genes.⁽⁴⁾ Exclusively chronic genes with enriched GO motifs, such as development and morphogenesis, also showed relatively high metrics, but for human NAFLD, recall and precision were lower than for the common genes.

In conclusion, our analyses led to the identification of genes that are similarly regulated in human and mouse liver disease. Although major species differences exist, the currently best available mouse models reach a recall of 0.4 and precision of 0.33 with respect to the genes significantly altered in human liver diseases.

Acknowledgment: The authors thank Ms. Hoyjin Kim for the graphic design of the experimental setups and Ms. Zaynab Hobloss and Ms. Lisa Brackhagen for the technical assistance. They also acknowledge Dr. Nachiket Vartak for the valuable advice and discussion of the manuscript, and Dr. Bence Szalai for the helpful discussions.

Data Availability Statement: The code to perform all presented analyses is written in R and is freely available on Github. Reproducibility of all analyses is ensured by the R package workflowr (version 1.6.2) by deploying all of our analysis scripts at a dedicated webpage. All data sets required to execute the code are available at Zenodo. The transcriptomics raw data of the here analyzed chronic and acute mouse models are available as superseries at GEO under accession number GSE166868.

REFERENCES

- 1) Younossi ZM, Stepanova M, Ong J, Trimble G, AlQahtani S, Younossi I, et al. Nonalcoholic steatohepatitis is the most rapidly increasing indication for liver transplantation in the United States. *Clin Gastroenterol Hepatol* 2021;19:580-589.e5.
- 2) Leist M, Hartung T. Inflammatory findings on species extrapolations: humans are definitely no 70-kg mice. *Arch Toxicol* 2013;87:563-567.
- 3) Teufel A, Itzel T, Erhart W, Brosch M, Wang XY, Kim YO, et al. Comparison of gene expression patterns between mouse models of nonalcoholic fatty liver disease and liver tissues from patients. *Gastroenterology* 2016;151:513-525.e0.
- 4) Campos G, Schmidt-Heck W, De Smedt J, Widera A, Ghallab A, Pütter L, et al. Inflammation-associated suppression of metabolic gene networks in acute and chronic liver disease. *Arch Toxicol* 2020;94:205-217.
- 5) Ghallab A, Myllys M, Holland CH, Zaza A, Murad W, Hassan R, et al. Influence of liver fibrosis on lobular zonation. *Cells* 2019;8:1556.
- 6) Ghallab A, Hofmann U, Sezgin S, Vartak N, Hassan R, Zaza A, et al. Bile microinfarcts in cholestasis are initiated by rupture of the apical hepatocyte membrane and cause shunting of bile to sinusoidal blood. *Hepatology* 2019;69:666-683.
- 7) Godoy P, Widera A, Schmidt-Heck W, Campos G, Meyer C, Cadenas C, et al. Gene network activity in cultivated primary hepatocytes is highly similar to diseased mammalian liver tissue. *Arch Toxicol* 2016;90:2513-2529.
- 8) Teske BF, Wek SA, Bunpo P, Cundiff JK, McClintick JN, Anthony TG, et al. The eIF2 kinase PERK and the integrated

- stress response facilitate activation of ATF6 during endoplasmic reticulum stress. *Mol Biol Cell* 2011;22:4390-4405.
- 9) Moylan CA, Pang H, Dellinger A, Suzuki A, Garrett ME, Guy CD, et al. Hepatic gene expression profiles differentiate presymptomatic patients with mild versus severe nonalcoholic fatty liver disease. *Hepatology* 2014;59:471-482.
 - 10) Hoang SA, Oseini A, Feaver RE, Cole BK, Asgharpour A, Vincent R, et al. Gene expression predicts histological severity and reveals distinct molecular profiles of nonalcoholic fatty liver disease. *Sci Rep* 2019;9:12541.
 - 11) **Ahrens M, Ammerpohl O**, von Schönfels W, Kolarova J, Bens S, Itzel T, et al. DNA methylation analysis in nonalcoholic fatty liver disease suggests distinct disease-specific and remodeling signatures after bariatric surgery. *Cell Metab* 2013;18:296-302.
 - 12) Horvath S, Erhart W, Brosch M, Ammerpohl O, von Schönfels W, Ahrens M, et al. Obesity accelerates epigenetic aging of human liver. *Proc Natl Acad Sci U S A* 2014;111:15538-15543.
 - 13) Ramnath D, Irvine KM, Lukowski SW, Horsfall LU, Loh Z, Clouston AD, et al. Hepatic expression profiling identifies steatosis-independent and steatosis-driven advanced fibrosis genes. *JCI Insight* 2018;3:120274.
 - 14) Garcia-Alonso L, Holland CH, Ibrahim MM, Turei D, Saez-Rodriguez J. Benchmark and integration of resources for the estimation of human transcription factor activities. *Genome Res* 2019;29:1363-1375.
 - 15) Holland CH, Szalai B, Saez-Rodriguez J. Transfer of regulatory knowledge from human to mouse for functional genomics analysis. *Biochim Biophys Acta Gene Regul Mech* 2019;1863:194431.
 - 16) Schubert M, Klinger B, Klünemann M, Sieber A, Uhlitz F, Sauer S, et al. Perturbation-response genes reveal signaling footprints in cancer gene expression. *Nat Commun* 2018;9:20.
 - 17) Sezgin S, Hassan R, Zühlke S, Kuepfer L, Hengstler JG, Spitteller M, et al. Spatio-temporal visualization of the distribution of acetaminophen as well as its metabolites and adducts in mouse livers by MALDI MSI. *Arch Toxicol* 2018;92:2963-2977.
 - 18) Ramachandran P, Dobie R, Wilson-Kanamori JR, Dora EF, Henderson BEP, Luu NT, et al. Resolving the fibrotic niche of human liver cirrhosis at single-cell level. *Nature* 2019;575:512-518.
 - 19) Thurman RG, Ji S, Lemasters JJ. Alcohol-induced liver injury. The role of oxygen. *Recent Dev Alcohol* 1984;2:103-117.
 - 20) Furuya S, Cichocki JA, Konganti K, Dreval K, Uehara T, Katou Y, et al. Histopathological and molecular signatures of a mouse model of acute-on-chronic alcoholic liver injury demonstrate concordance with human alcoholic hepatitis. *Toxicol Sci* 2019;170:427-437.
 - 21) Tsuchida T, Lee YA, Fujiwara N, Ybanez M, Allen B, Martins S, et al. A simple diet- and chemical-induced murine NASH model with rapid progression of steatohepatitis, fibrosis and liver cancer. *J Hepatol* 2018;69:385-395.
 - 22) Jansen PLM, Ghallab A, Vartak N, Reif R, Schaap FG, Hampe J, et al. The ascending pathophysiology of cholestatic liver disease. *Hepatology* 2017;65:722-738.
 - 23) **Ramirez Flores RO, Lanzer JD**, Holland CH, Leuschner F, Most P, Schultz J-H, et al. Consensus transcriptional landscape of human end-stage heart failure. *J Am Heart Assoc* 2021;10:e019667.
 - 24) Michel K, Roth S, Trautwein C, Gong W, Flemming P, Gressner AM. Analysis of the expression pattern of the latent transforming growth factor beta binding protein isoforms in normal and diseased human liver reveals a new splice variant missing the proteinase-sensitive hinge region. *Hepatology* 1998;27:1592-1599.
 - 25) Chen J, Gao G, Wang H, Ye X, Zhou J, Lin J. Expression and clinical significance of latent-transforming growth factor beta-binding protein 2 in primary hepatocellular carcinoma. *Medicine* 2019;98:e17216.

Author names in bold designate shared co-first authorship.

Supporting Information

Additional Supporting Information may be found at onlinelibrary.wiley.com/doi/10.1002/hep4.1797/supinfo.